

# Computer Simulation of a Hardness Indent Test into Nickel Nano Thin Films

Edward Parker and Peter Gaudreau

Virginia Polytechnic Institute and State University, Department of Materials Science and Engineering  
Blacksburg, VA 24060

## Abstract

Current experiments suggest that mechanical properties of thin films are different at thicknesses less than 100 nm. In this study, embedded atom method computer simulations are used to examine the differences in strengthening mechanisms at the nano scale. The simulation shows the mechanisms responsible for the differences in hardness with varying sample thicknesses from 12.8, 8, 6, and 4 nm. The simulation results show that as film thickness decreases the hardness of the film increases. Simulations were performed in single crystal films as well as model tricrystals in order to study the effects of the grain boundaries. Tricrystalline films emitted dislocations at a lower pressure than single crystals.

Keywords: Embedded atom method, molecular dynamics, indentation, hardness, nickel, nano, thin film, visualization

## 1. Introduction: Behavior of Thin Films at Nano Scale

Thin films are used in several applications, including light emitting diodes (LED's), solar panels, and computer circuitry. Mechanical properties of thin films, such as hardness, are of concern when considering real world applications because mechanical properties of thin films are affected by point defects, dislocations, and grain size.<sup>[1]</sup> For example, the Hall Petch effect relates material strengthening with decreasing grain size. At the macro scale the strength of the material increases as the diameter of the grains decrease. However, this relationship between grain size and strength is lost when the grain diameter approaches the nano scale, grain sizes less than 20 nm.<sup>[2]</sup>

To completely understand nano scale behavior computer simulations are used to model atomic motions that occur during many different kinds of mechanical deformation in metals, including tensile tests and compressive loading scenarios.<sup>[3]</sup> At this point, however, there have been no attempts to model a hardness indentation on tricrystalline nickel nano thin films with varying film thickness. A tricrystalline film describes a polycrystalline film that has three grains with similar structure within the sample. The benefit of simulating the indentation is the visualization of atomic motions and dislocations as a function of time. The simulation also provides information on the mechanisms responsible for the differences between hardness

data of nano scale versus macro scale film thicknesses. In this work we address 1) the response of single crystals films of varying thicknesses and 2) the effect of low angle boundaries present in the indented films.

## 2. Theory: Embedded Atom Method

The embedded atom method is currently a common technique used in computer simulation of metal systems.<sup>[4-7]</sup> The method provides a description of the interatomic forces in the system. It calculates the interatomic potentials in metals and models forces between atoms as follows:

$$E = \frac{1}{2} \sum_{i,j} V(r_{ij}) + \sum_i F(r_i) \quad (1)$$

where  $E$  is the total energy of the system,  $V(r_{ij})$  represents the energy between an atom and its nearest neighboring atom, and  $F(r_i)$  represents an embedding function responsible for free electrons in the metal.<sup>[5-7]</sup> The nickel system is a face centered cubic (FCC) lattice.<sup>[1]</sup> The potentials reproduce the perfect lattice properties and were developed by Y. Mishin et al.<sup>[8]</sup>

### 3. Procedure

#### 3.1 Computer Simulation Techniques

Simulating mechanical deformation in real time requires a vast number of calculations; therefore, powerful computer software is required for the simulation of a hardness test. A program called Lammmps is currently being used for simulating materials using the embedded atom method.<sup>[3]</sup> These simulations can show applied forces to the lattice and the subsequent atomic motions from the deformation. Lammmps is capable of mapping the Cartesian coordinates (x,y,z) of millions of atoms in real time. However, to view the atoms a visualization program called Amira is used in combination with the Lammmps code. The Lammmps code is modified to establish different film thicknesses and generates the coordinates for the atoms in real time, and Amira shows the atoms in motion, making it possible to view dislocation propagation, and grain boundary interactions associated with the applied force from the hardness test.<sup>[9]</sup>

#### 3.2 Crystal Growth

To observe the hardness indent on a thin film, the different nickel films was simulated using the Voronoi grain growth method. This method is a program used to nucleate grains in a metal system utilizing the Y. Mishin EAM potential for nickel.<sup>[8]</sup> Several different grain structures were created for this experiment. Films were created as single grain perfect crystals, and crystals with three grains and varying misorientation angles of 5° and 10°. The dimensions of the film are 25nm in the  $[1\bar{1}0]$  direction and 25 nm in the  $[11\bar{2}]$  direction. Once the grains are nucleated, the internal stresses and grain boundar-

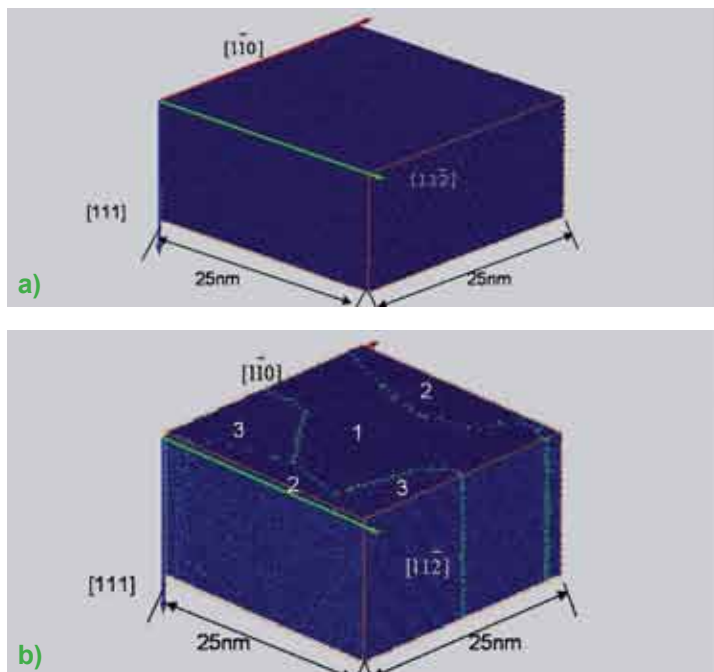


**Figure 1.** Structure and orientation of 12.8 nm a) single crystal and b) 10° tricrystal

ies are relaxed at 300 K by using the Lammmps code. The final result of the relaxation is a tricrystalline nickel and single crystal thin film at ambient pressures between 0 and 100 bar. Figure 1 shows the structure and orientation of the relaxed samples used for indentation. The film surfaces are oriented normal to the  $[111]$  direction.

#### 3.3 Indentation Simulation

The next step is to simulate a hardness indent into the thin films using the Lammmps code. A hardness indenter with a radius of 30.3 nm was chosen. The Lammmps code is written to simulate the lowering of the indenter down the Z  $[111]$  direction into the various thin films. The optimal loading rate for observing the entire indentation process is 10 m/s. The force and atomic positions are outputs at 5 ps or 10 ps intervals until the hardness indent is completed after the tip travels a depth equal to 20% of the overall thickness. The simulation is performed at 300 K with the bottom surface as a fixed boundary condition in the  $[111]$  direction and periodic in the  $[1\bar{1}0]$  and  $[11\bar{2}]$  directions. The atoms in the fixed region are actually allowed to move within the (111) plane, but not along the  $[111]$  direction. The atomic positions are entered into visualization software (Amira) in order to view the indentation process in real time 3-D visualization. Forces from the indenter are obtained during the experiment. The contact area is also calculated from the atomic positions and is used to obtain contact pressures.

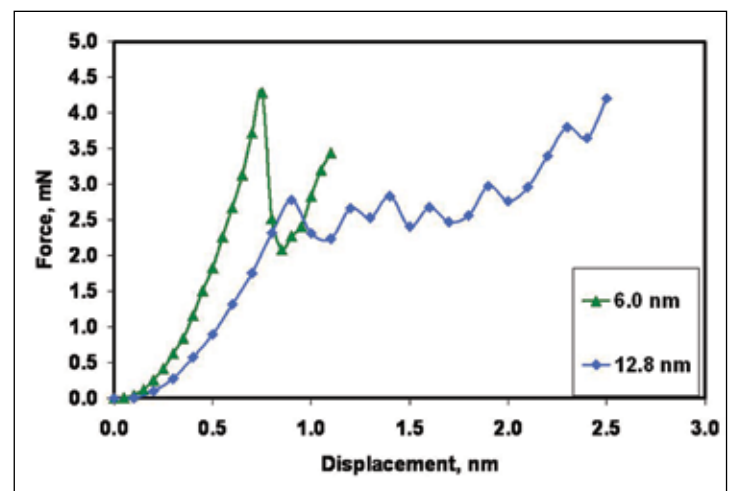


**Figure 2.** Force (N) vs. displacement (nm)

### 4. Results and Discussion

#### 4.1 Effect of Film Thickness

Figure 2 shows the effect of thickness on the force displacement curves characteristic of the films. Figure 3 shows the simulated indentation of thin films of 6.0 nm and 12.8 nm, and Figure 4 shows the contact pressure of the indenter on the film surface for different values of film thickness. The trend that is observed is that the film thickness decreases the slope

of the elastic response of the film increases. The visualization of the hardness indent showed the mechanisms responsible for the trends found in the previous graphs. Figure 2 shows the dislocation loops that were observed during the visualization of 6.0 nm and 12.8 nm sample.

In the elastic part of the indentation different slopes of the pressure versus indentation depth are observed for varying film thicknesses. However, the contact pressure necessary for the initiation of plasticity in the single crystal films is independent of the film thickness. Differences in the loops configuration are observed in the plastic part of the indentation. As the film

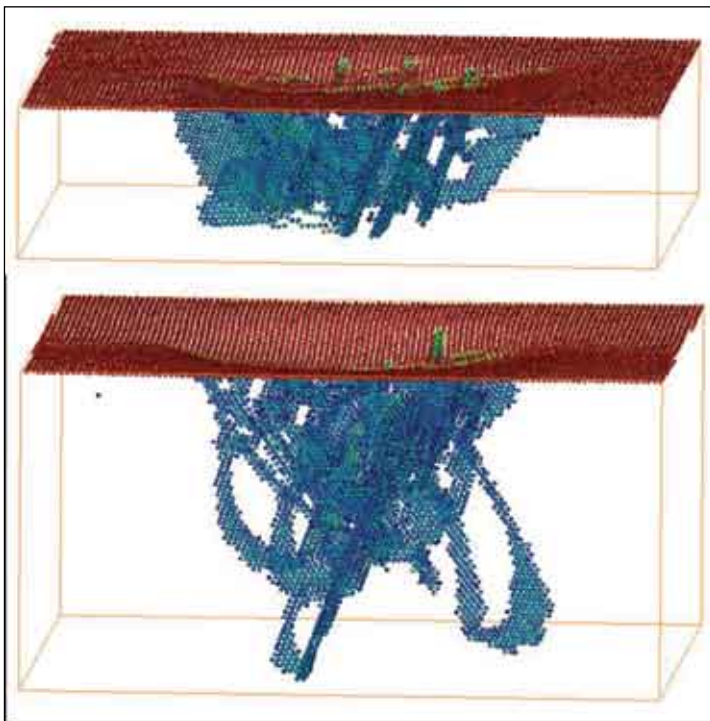


**Figure 3.** Indentation of 6.0 nm film and 12.8 nm film at equivalent pressure of 38.10 GPa

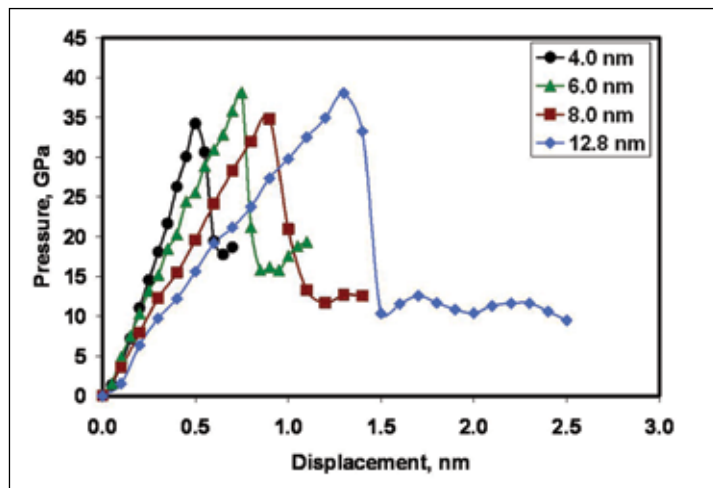


**Figure 4.** Pressure (GPa) vs. displacement (nm) of single crystal varying sample thickness

thickness decreases, loops can not move as easily due to the fact that the space available for the dislocation loop is smaller. This impediment of formation and motion of dislocation loops leads to hardening of the material.

#### 4.2 Effect of Grain Boundaries

From the pressure versus displacement graphs shown in Figure 3, films containing grain boundaries with misorientations of 5 and 10 degrees were used. The grain boundary planes were oriented perpendicular to the film surface. The initial linear region within the graph correlates to the elastic response of the films and the peaks correlate to the first dislocation emission. The films containing grain boundaries emit dislocations at lower contact pressures than single crystal. The higher pressures in the single crystal are due to the lack of defects within the system.

#### 4.3 Dislocation Emitting Sites

The pressure versus displacement graphs shown in Figure 4 were studied along with the visualization of the sample to see where the dislocations were emitted. There were two locations where the dislocations initially were emitted: from the grain boundary or underneath the indenter. This comparison provided more understanding of the trend of higher pressure to emit the first dislocation in a single crystal than the lower pressure in a tricrystal, shown in Figure 5. Examples of the emitting sites are shown in Figure 6. In most cases for the tricrystalline films the dislocations emitted from initial defects. However, in some of the thinner tricrystalline films there were dislocations emitted in areas of the film with no defects. For these very thin films (40 nm) the grain boundaries were not effective emission sites for the dislocations. For the relatively thicker films the dislocations were emitted from the grain boundaries. In the single crystal films there were no initial defects and the first dislocation emitted from directly underneath the indenter every time.

#### 4.4 Differences at the Nano Scale

One of the important reasons for simulation of nickel films was to view the different hardening effects at the nano scale. To summarize our results, Figure 7 shows that the elastic response (slope of pressure curve) is stronger, indicating much harder films at low thicknesses. Figure 7 also shows as film thickness increases, the hardness of the film begins to approach bulk hardness values. As the thickness of the film increases, another trend is apparent. Figure 8 shows that as film thickness increases, the effect of preexisting grain boundaries is stronger. In very thin films, the difference between a single crystal film and a tricrystal film is not as pronounced. In the larger films, the initial defects provide sources to form larger loops. In the smaller films these sources are still present in the tricrystalline

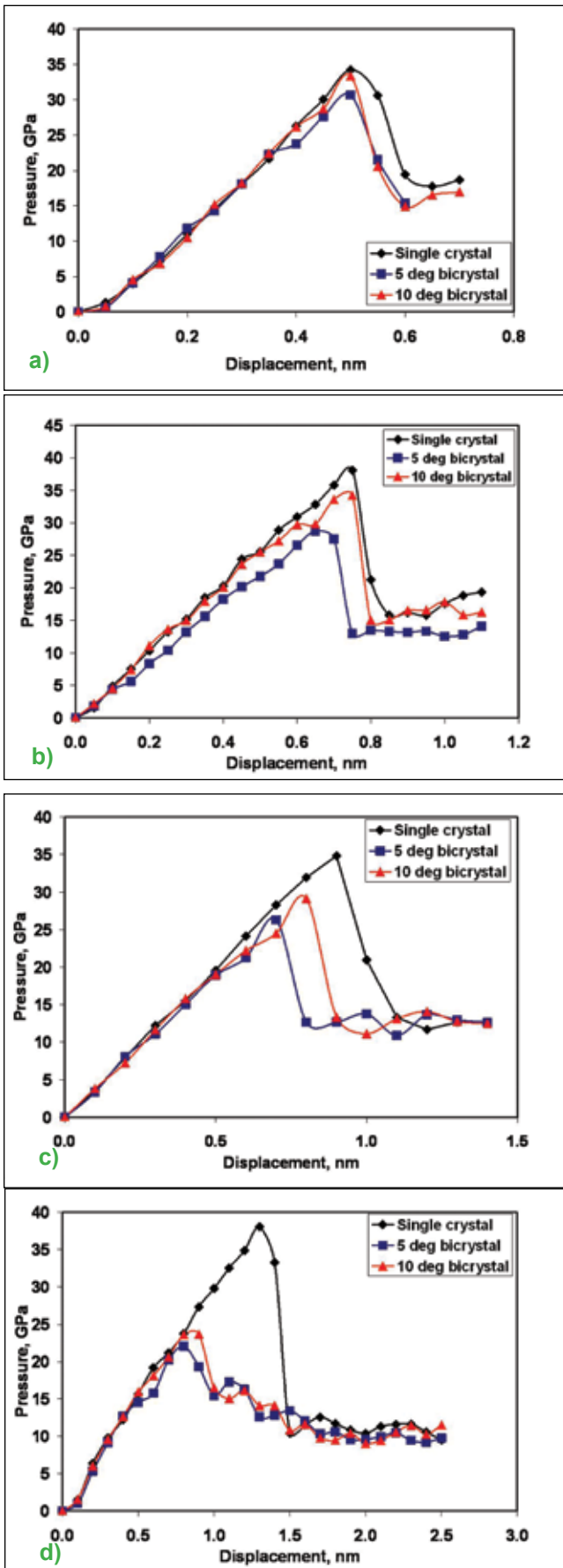


Figure 5. Pressure vs. displacement at a) 4 nm b) 6 nm c) 8 nm and d) 12.8 nm

films; however, there is not enough space between the surfaces of the film to generate a dislocation loop, this is caused by the size dependence from equation that follows:

$$s^* = mb^2 / (2L) \tag{2}$$

This equation shows the critical stress of emitting a pure edge dislocation, where  $\mu$  is the shear modulus of nickel with the value of 760 MPa, the burger's vector  $b = 2.5 \text{ \AA}$  and  $L$  the length of the dislocation loop.<sup>[10]</sup>

### 5. Conclusions

In the simulation of hardness indent into a nickel nano thin film the hardness increases with decreasing film thicknesses. One hardening mechanism with decreasing film thickness was the added constraint on the formation and motion of

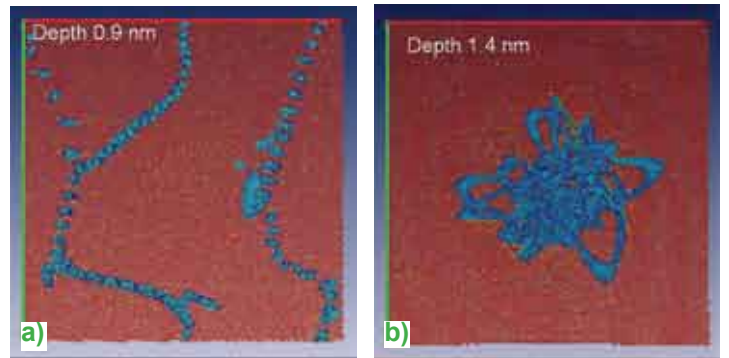


Figure 6. Emission of first dislocations in 12.8 nm thick film: a) 10deg bicrystal at a depth of 0.9 nm and pressure of 23.68 GPa b) single crystal at a depth of 1.4 nm and pressure of 33.28 GPa

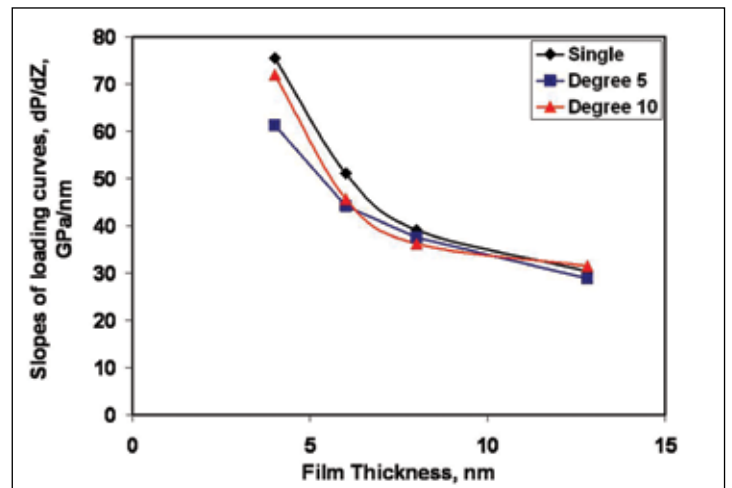
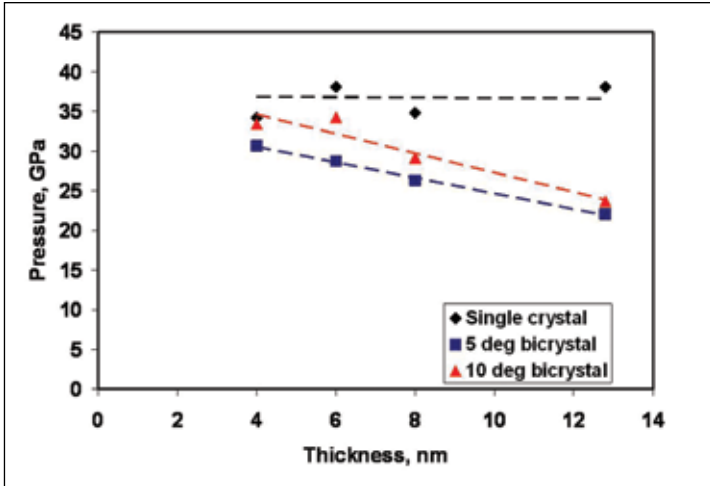


Figure 7. Slopes of loading curves vs. film thickness



**Figure 8.** Peaks of loading curves vs. film thickness

dislocation loops. Hardness increases with decreasing thickness because there is less room for dislocation loops making it more difficult for the lattice to deform plastically.

In the simulation of a hardness indent into a nickel nano thin film the films with initial grain boundaries are not as hard as the single crystal films. This is to be expected because initial defects in the lattice provide sites for dislocation emission. In thicker films the presence of initial defects has a greater effect on hardness than in thinner films because the length between surfaces effects the emission of dislocation loops. As the radius of a dislocation loop increases, the force needed to emit the loop decreases.

### Acknowledgements

We would like to acknowledge Dr. Farkas of Virginia Tech, graduate student Joshua Monk of Virginia Tech and graduate student Donald Ward of Brown University; for helping us in this project.

### References

- [1] Callister, William D. *Materials Science and Engineering, an Introduction*, Wiley, 2003.
- [2] Cordill, M.J., Chambers, M. D., Lund, M. S., Hallman, D. M., Perry, C. R., Carter, C. B., Bapat, A., Kortshagen, U., Gerberich, W. W. *Plasticity Response in Ultra-Small Confined Cubes and Films*. 2005.
- [3] Plimpton, S. J., Lammmps Code, *Journal of Computational Physics*, 117, 1-19, **1995**, [www.cs.sandia.gov/~sjplimp/lammmps.html](http://www.cs.sandia.gov/~sjplimp/lammmps.html)
- [4] Finnis, Mike. *Interatomic Forces in Condensed Matter*. Oxford University Press, 2003, p 129-186.

- [5] Hyde, Brian. *Effects of Carbon on Fracture Mechanisms in Nanocrystalline BCC Iron – Atomistic Simulations*, Virginia Tech Dissertation 2004, p 6-18
- [6] Xie, Zhao-Yang. *Atomistic Simulation of Dislocations Core Structures in B<sub>2</sub> NiAl* Virginia Tech Dissertation Dec. 1993, p 9-13.
- [7] Cabral Cardozo, Antonia Fernando. *Computer Simulation of Grain Boundary Multiplicity in Ni<sub>3</sub>Al*. Virginia Tech Dissertation April 1991, p 12-17.
- [8] Mishin, Y.; Mehl, M. J.; Papaconstantopoulos, D. A.; Embedded-atom potential for B<sub>2</sub>-NiAl, *Physical Review B* 65, **1984**.
- [9] [www.amiravis.com](http://www.amiravis.com)
- [10] Hirth, J.P; and Lothe, J. *Theory of Dislocations*. John Wiley & Sons, Inc. 1982.
- [11] Deak, Peter; Frauenheim, Thomas; and Pederson, Mark R. *Computer Simulation of Materials at Atomic Level*. Wiley-VCH, 2000

### About the Authors



*Edward Parker*

Edward Parker, originally from Raleigh, North Carolina, graduated from the Materials Science and Engineering program at Virginia Tech in the spring of 2006 with a bachelor degree. He obtained a job as a process engineer with Cree Inc. of Raleigh, NC, working with LED lighting.



*Peter Gaudreau*

Peter Gaudreau, originally from Woonsocket, Rhode Island, also graduated from the Materials Science and Engineering program at Virginia Tech in the spring of 2006 with a bachelor degree. He obtained a job shortly after graduation in Riverdale, Illinois as a metallurgist working with Mittal Steel.